

Manganese Redistribution by Calcium-stimulated Vesicle Trafficking Bypasses the Need for P-type ATPase Function^{*[5]}

Received for publication, October 21, 2014, and in revised form, February 17, 2015. Published, JBC Papers in Press, February 20, 2015, DOI 10.1074/jbc.M114.616334

Néstor García-Rodríguez^{†1}, Javier Manzano-López^{§2}, Miguel Muñoz-Bravo[‡], Elisabet Fernández-García[‡], Manuel Muñiz[§], and Ralf Erik Wellinger^{‡3}

From the [†]Centro Andaluz de Biología Molecular y Medicina Regenerativa (CABIMER), Universidad de Sevilla, 41092, Sevilla, Spain and the [§]Departamento de Biología Celular–Instituto de Biomedicina de Sevilla (IBiS), Universidad de Sevilla, 41012 Sevilla, Spain

Background: Yeast is a model system for the study of mechanisms governing eukaryotic Golgi-Mn²⁺ homeostasis.

Results: We provide evidence that calcium stimulates ER and late endosome/*trans*- to *cis*-Golgi manganese delivery and bypasses the need for Pmr1.

Conclusion: Vesicle trafficking promotes organelle-specific ion interchange and cytoplasmic metal detoxification.

Significance: Our findings open new perspectives on chemical modifiers of Hailey-Hailey disease.

Regulation of intracellular ion homeostasis is essential for eukaryotic cell physiology. An example is provided by loss of *ATP2C1* function, which leads to skin ulceration, improper keratinocyte adhesion, and cancer formation in Hailey-Hailey patients. The yeast *ATP2C1* orthologue *PMR1* codes for a Mn²⁺/Ca²⁺ transporter that is crucial for *cis*-Golgi manganese supply. Here, we present evidence that calcium overcomes the lack of Pmr1 through vesicle trafficking-stimulated manganese delivery and requires the endoplasmic reticulum Mn²⁺ transporter Spf1 and the late endosome/*trans*-Golgi Nramp metal transporter Smf2. Smf2 co-localizes with the putative Mn²⁺ transporter Atx2, and *ATX2* overexpression counteracts the beneficial impact of calcium treatment. Our findings suggest that vesicle trafficking promotes organelle-specific ion interchange and cytoplasmic metal detoxification independent of calcineurin signaling or metal transporter re-localization. Our study identifies an alternative mode for *cis*-Golgi manganese supply in yeast and provides new perspectives for Hailey-Hailey disease treatment.

The intracellular levels of ions and other micronutrients are closely regulated in eukaryotic cells. This is the case for the trace element manganese (Mn²⁺), whose regulation is particularly important. This redox active metal is a key cofactor for a wide range of enzymes located in every cellular compartment (1). However, at high concentrations Mn²⁺ is toxic and promotes DNA damage coupled to replication defects in yeast (2). In humans, overexposure to Mn²⁺ results in a neurological syn-

drome called manganism, whose symptoms resemble those of Parkinson disease (3). In addition, Mn²⁺ has been shown to favor prion misfolding if it displaces copper as the protein cofactor (4). Hailey-Hailey disease phenotypes have been associated with mutations affecting calcium and/or manganese transport activities of the Golgi Ca²⁺/Mn²⁺ transporter *ATP2C1* (5). A representative Hailey-Hailey phenotype caused by alterations in the intracellular Mn²⁺ flux includes keratinocyte differentiation (6). For these reasons, revealing the intracellular mechanisms that regulate Mn²⁺ homeostasis pathways is of clinical importance.

Much of our current understanding of eukaryotic manganese homeostatic mechanisms comes from the budding yeast, *Saccharomyces cerevisiae*. Yeast Mn²⁺ uptake is provided by the plasma membrane transporter Smf1, a member of the natural resistance-associated macrophage protein (Nramp)⁴ family (7). Smf2 represents a member of intracellular Nramp Mn²⁺ transporters essential for the activity of Mn²⁺-dependent enzymes, which include the mitochondrial Sod2 protein and Golgi-hosted sugar transferases (8). Smf2 localizes to Golgi-like vesicles, and a drop in whole-cell Mn²⁺ has been observed upon *SMF2* deletion (8). Under physiological conditions, ~90% of newly synthesized Smf1 and Smf2 are directly targeted to the vacuole for degradation, presumably to limit uptake of toxic Mn²⁺ amounts (9, 10). When Mn²⁺ becomes limiting, these transporters are delivered to the cell surface (Smf1) and intracellular vesicles (Smf2) to increase Mn²⁺ uptake (9, 10). In contrast, in conditions of toxic metal concentrations, the vacuolar degradation of the Nramp transporters is enhanced, and Smf1 is virtually eliminated from the plasma membrane (11). Moreover, Mn²⁺ uptake by manganese-phosphate complexes is facilitated by the high affinity cell surface phosphate transporter Pho84 (12).

Other factors that influence intracellular Mn²⁺ homeostasis include the putative Mn²⁺ transporter Atx2. Atx2 localizes to Golgi-like vesicles, but the mechanism by which Atx2 regulates

* This work was supported by grants from the Spanish Ministry of Science and Innovation (BFU2010-21339) and the Junta de Andalucía-European Union (08-CTS-04297 and P11-CTS-7962) (to R. E. W.) and by a grant from the Spanish Ministry of Science and Innovation (BFU2011-24513) and the Junta de Andalucía (P09-CVI-4503) (to M. M.).

[5] This article contains supplemental data.

¹ Recipient of a pre-doctoral training grant from the University of Seville/El Monte Foundation.

² Recipient of a pre-doctoral training grant from the University of Seville.

³ To whom correspondence should be addressed: Dept. of Molecular Biology, Centro Andaluz de Biología Molecular y Medicina Regenerativa (CABIMER), Universidad de Sevilla, Av Américo Vespucio s/n, 41092, Sevilla, Spain. Tel.: 34-954467789, Fax: 34-954461664; E-mail: ralf.wellinger@cabimer.es.

⁴ The abbreviations used are: Nramp, natural resistance-associated macrophage protein; CFW, calcofluor white; CPY, carboxypeptidase Y; ER, endoplasmic reticulum; SC, Synthetic Complete; YPAD, yeast peptone adenine dextrose.

TABLE 1
Yeast strains and plasmids used in this study

Strain or plasmid	Relevant genotype or description	Source
Strains		
BY4741	<i>MAT a ura3Δ0 leu2Δ0 his3Δ0 met15Δ0</i>	EUROSCARF
BY4742	<i>MAT α ura3Δ0 leu2Δ0 his3Δ0 lys2Δ0</i>	EUROSCARF
NGY051	<i>BY4741 pmr1Δ::kan</i>	(2)
NGY178	<i>MAT α ura3Δ0 leu2Δ0 his3Δ0 met15Δ0 lys2Δ0 pmr1Δ::nat</i>	This study
YML123C	<i>BY4741 pho84Δ::kan</i>	EUROSCARF
NGY223	<i>MAT α ura3Δ0 leu2Δ0 his3Δ0 met15Δ0 pmr1Δ::nat pho84Δ::kan</i>	This study
YHR050W	<i>BY4741 smf2Δ::kan</i>	EUROSCARF
NGY183	<i>MAT α ura3Δ0 leu2Δ0 his3Δ0 met15Δ0 lys2Δ0 pmr1Δ::nat smf2Δ::kan</i>	This study
YDL128W	<i>BY4741 vcx1Δ::kan</i>	EUROSCARF
NGY192	<i>BY4741 pmr1Δ::nat vcx1Δ::kan</i>	This study
YGR217W	<i>BY4741 cch1Δ::kan</i>	EUROSCARF
NGY190	<i>MAT a ura3Δ0 leu2Δ0 his3Δ0 met15Δ0 lys2Δ0 pmr1Δ::nat cch1Δ::kan</i>	This study
YLR220W	<i>BY4741 ccc1Δ::kan</i>	EUROSCARF
NGY193	<i>MAT α ura3Δ0 leu2Δ0 his3Δ0 met15Δ0 pmr1Δ::nat ccc1Δ::kan</i>	This study
NGY233	<i>MAT a leu2Δ0 his3Δ0 met15Δ0 trp1Δ0</i>	This study
	<i>SMF2-GFP- CaURA3</i>	
NGY234	<i>MAT α leu2Δ0 his3Δ0 met15Δ0 trp1Δ0 lys2Δ0</i>	This study
	<i>SMF2-GFP- CaURA3 pmr1Δ::kan</i>	
YOL122C	<i>BY4741 smf1Δ::kan</i>	EUROSCARF
NGY222	<i>MAT a ura3Δ0 leu2Δ0 his3Δ0 met15Δ0 lys2Δ0 pmr1Δ::nat smf1Δ::kan. Grown in the presence of 10 mM CaCl₂</i>	This study
NGY241	<i>MAT α ade2-1 ura3-1 pmr1Δ:: HIS3 cnb1Δ::LEU2</i>	This study
YOL018C	<i>BY4741 tlg2Δ::kan</i>	EUROSCARF
NGY208b	<i>BY4741 pmr1Δ::nat tlg2Δ::kan</i>	This study
RH1737	<i>MAT a ura3Δ0 leu2Δ0 his4Δ0 bar1-1 sec18-20</i>	H.Riezman
NGY230	<i>MAT a ura3Δ0 leu2Δ0 pmr1Δ::kan sec18-20</i>	This study
YEL036C	<i>BY4741 anp1Δ::kan</i>	EUROSCARF
Plasmids		
p2UGpd	2-μm origin, <i>URA3</i> , <i>GPDp</i>	(27)
pATX2	p2UGpd, <i>GPDp-ATX2</i>	(2)
pTPQ127	<i>CEN, LEU2, GPDp-FYVE-dsRed</i>	(70)
pTPQ128	<i>CEN, LEU2, ADH1p-SEC7-dsRed</i>	(70)
Pv2-dsRed-PEP12	pRS414, <i>TRP1, PHO5p-dsRed-PEP12</i>	(71)
RH3100	<i>TRP1, mRFP-SED5</i>	(72)
pNG011	pUG23, <i>METp-SMF2-GFP</i>	This study
pNG026	p2UGpd, <i>GPDp-ATX2-mCherry</i>	This study
pRS315-HA-GFP-cSNC1	<i>CEN, LEU2, HA-GFP-cSNC1</i>	(53)

intracellular Mn²⁺ levels remains unknown (13). Recently, the P-type ATPase Spf1 (*hATP13A1*) has been suggested to regulate Mn²⁺ transport into the endoplasmic reticulum (ER) (14), whereas Pmr1, a Golgi-localized P-type Ca²⁺ and Mn²⁺ ATPase, pumps cytosolic Mn²⁺ into the lumen of the Golgi (15–17). Apart from providing sugar transferases with Mn²⁺ as cofactor, Pmr1 has another role in Mn²⁺ detoxification by secretory pathway-mediated excretion (16–18). In addition to Pmr1, Mn²⁺ detoxification can be carried out by the vacuolar iron and manganese transporter Ccc1 (19).

Membrane fission and fusion are essential processes, allowing the dynamic communication between membrane-bounded organelles in all eukaryotic cells. Lipid vesicles are constantly emerging from one membrane to fuse with another, providing transport shuttles between distinct intracellular compartments. Increasing evidence suggests that calcium (Ca²⁺) plays a role in the regulation of membrane trafficking. For example, Ca²⁺ appears to be involved in ER to Golgi transport (20), intra-Golgi transport (21), and early endosome fusion (22) as well as yeast homotypic vacuole fusion (23).

Although many players involved in the intracellular manganese trafficking network have been characterized in yeast, our understanding of organelle-to-organelle Mn²⁺ flux is far from complete. Here, we report a Pmr1-independent mechanism for cis-Golgi Mn²⁺ supply. This supply depends on the ER Mn²⁺ transporter Spf1 and the Smf2 late endosome/trans-Golgi Mn²⁺ transport activity and can be counteracted by *ATX2* overexpression. In addition, it requires extracellular CaCl₂ in

order to stimulate vesicle trafficking and membrane fusion. Based on our observations we propose a model on intracellular manganese homeostasis that provides mechanisms for intracellular ion flux and manganese detoxification.

EXPERIMENTAL PROCEDURES

Yeast Strains and Plasmids—Yeast strains and plasmids used in this study are listed in Table 1. Gene deletions were constructed by PCR-based methods using pAG25 (EUROSCARF) and pFA6a-*kLEU2MX6* (kindly provided by B. Pardo) as template plasmids. In other cases strains were derived from genetic crosses. The chromosomal *SMF2* open reading frame under the control of its own promoter was C-terminal-tagged with enhanced GFP (eGFP) by a PCR-based method using the tagging vector pKT209 (pFA6a-link-yEGFP-*CaURA3*) (24) as the template plasmid. To generate plasmid pNG011, *SMF2* was amplified from genomic DNA, digested with *EcoRI/SalI*, and inserted into *EcoRI/SalI* site of pUG23 (25). To generate plasmid pNG026, *ATX2* and mCherry were amplified from genomic DNA or pKS39 (26), respectively, using overlapping oligonucleotides. The PCR products were mixed and amplified using external oligonucleotides, digested with *BamHI/SacI*, and inserted into *BamHI/SacI* site of p2UGpd (27).

Drug Sensitivity Assays—Yeast cells were adjusted in concentration to an initial A₆₀₀ of 0.2, then serially diluted 1:10 and spotted onto plates without or with different drugs at the indicated concentrations (see figure legends). CaCl₂ was added when indicated. Plates were then incubated at 30 °C for 3–4

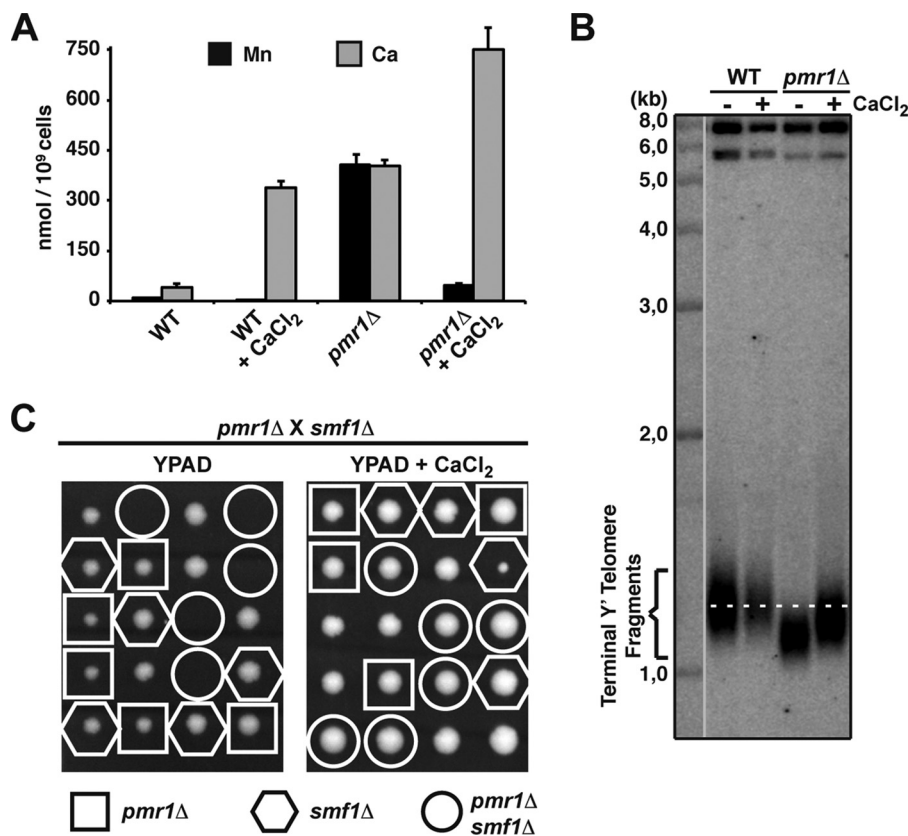


FIGURE 1. Intracellular Mn²⁺ levels decrease upon CaCl₂ addition. *A*, Addition of extracellular CaCl₂ reduces whole cell manganese content in *pmr1*Δ cells. Accumulation of manganese (Mn) and calcium (Ca) in WT and *pmr1*Δ cells without or with the addition of CaCl₂ (10 mM) was determined by inductively coupled plasma atomic emission spectrometry as described under "Experimental Procedures." Error bars represent S.D. *B*, CaCl₂ restores WT telomere length in *pmr1*Δ mutants. WT and *pmr1*Δ cells were grown in YPAD without or with the addition of 10 mM CaCl₂ for 3 days. Genomic DNA was isolated from the strains, digested with XhoI, and subjected to Southern blot (see "Experimental Procedures"). The location of the terminal Y' telomere fragments is indicated. The dashed white line marks the telomere size of WT. *C*, extracellular CaCl₂ bypasses *pmr1*Δ *smf1*Δ lethality. Shown is tetrad analysis crossing *pmr1*Δ with *smf1*Δ without (left) or with (right) 10 mM CaCl₂ in the medium. The genotype of the relevant spores is indicated.

days, except for temperature-sensitive mutants, which were incubated at the corresponding permissive or semipermissive temperatures.

Pulse-Chase Analysis of CPY—Pulse-chase labeling and analysis of immunoprecipitates was done as described previously (28).

Analysis of Telomere Length—Genomic DNA was isolated from yeast strains grown in YPAD for 3 days with or without the addition of 10 mM CaCl₂. DNA was digested with XhoI, separated on a 1% agarose-Tris borate EDTA gel, transferred to a Hybond XL (Amersham Biosciences) membrane, and hybridized with a ³²P-labeled DNA probe specific for the terminal Y' telomere fragment. The probe was generated by random hexanucleotide-primed DNA synthesis using a short Y' specific DNA template, which was generated by PCR from genomic yeast DNA using the primers Y' up (5'-TGCCGTGCAACAA-ACACTAAATCAA-3') and Y' low (5'-CGCTCGAGAAAGT-TGGAGTTTTTCA-3'). Three independent colonies of each strain were analyzed to ensure reproducibility.

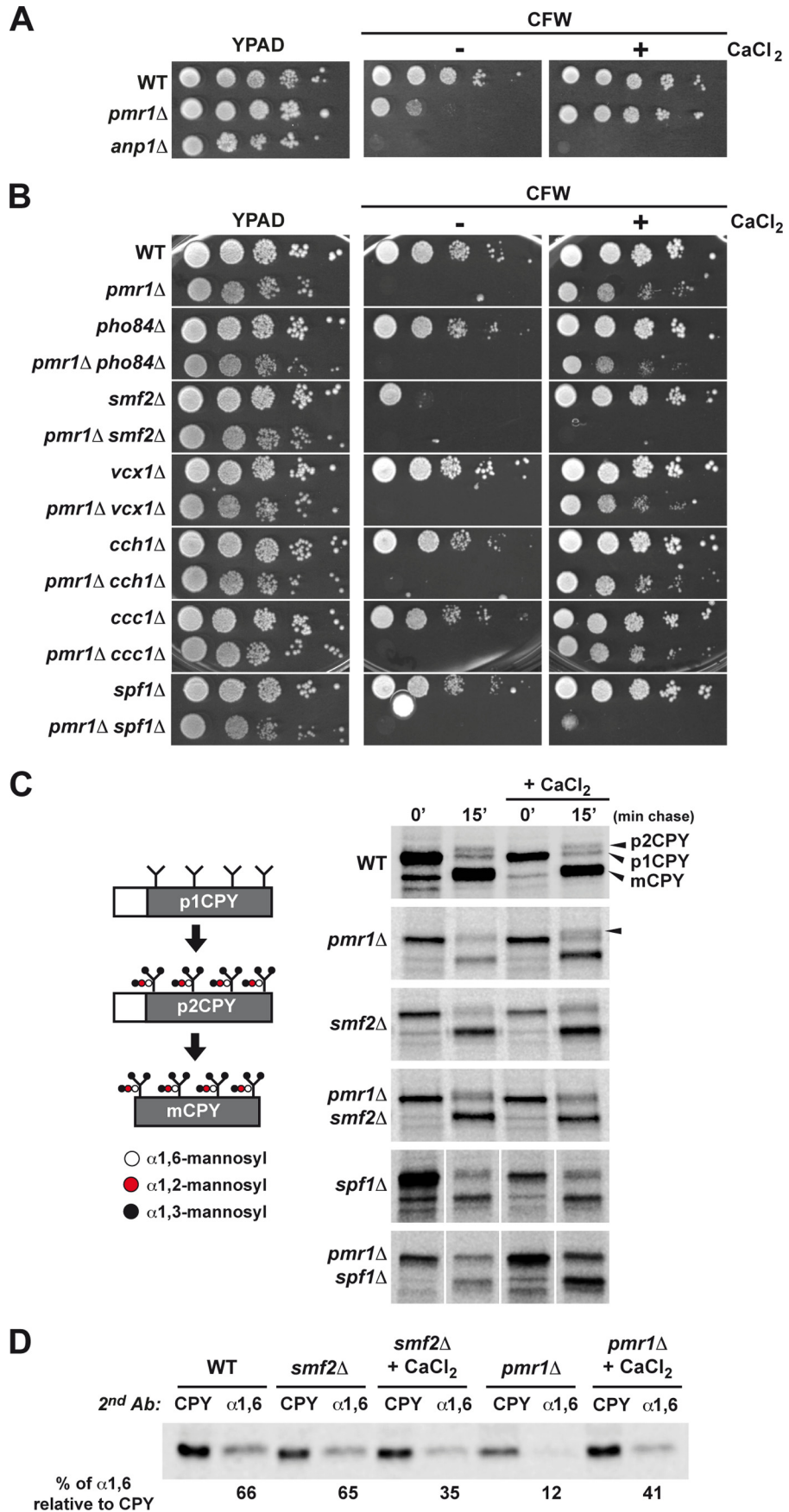
Fluorescence Microscopy—Plasmid harboring yeast cells were grown to mid-log-phase in selective Synthetic Complete (SC) medium to maintain the plasmid and fixed in 2.5% formaldehyde and 0.1 M potassium phosphate buffer, pH 6.4, for 10 min. Cells were then washed twice with 0.1 M potassium phosphate buffer, pH 6.6, and finally resuspended in 0.1 M potassium phos-

phate buffer, pH 7.4. Cells were imaged at 25 °C using a microscope (DM-6000B, Leica) at 100× magnification using L5, N3, and TX2 filters and a digital charge-coupled device camera (DFC350, Leica). Images were taken using LAS AF software (Leica) with the same exposure times for Smf2-GFP (1s) and lower exposure times for different marker proteins in the colocalization analysis. Images were assembled in Photoshop (Adobe) with only linear adjustments. Statistical analysis of colocalization was performed by counting at least 100 cells per marker derived from three independent experiments. Data are shown as the mean ± S.D.

Metal Measurements—Yeast cells were grown to an A₆₀₀ of 2.5 in YPAD medium or the same medium supplemented with 5 mM CaCl₂. In both cases the growth media was supplemented with 20 μM MnCl₂ to monitor metal accumulation under manganese toxicity conditions. The cultures were harvested and washed with TE (10 mM Tris-HCl and 1 mM EDTA, pH 8), then deionized water, and finally dried. Samples were subjected to acid digestion and applied to an ICP Horiba Jobin Yvon Ultima 2 atomic-emission spectrometer at the Microanalysis Service of University of Seville (Seville, Spain). Manganese and calcium content were measured according to the manufacturer's specifications.

Microarray Analysis—Gene expression profiles were determined by using the "3'-expression microarray" technology by

Intra-Golgi Manganese Redistribution



Affymetrix platform at the Genomics Unit of CABIMER (Seville, Spain) as described previously (2), with the modification that total RNA was isolated from cultures grown on YPAD + 5 mM CaCl₂.

RESULTS

CaCl₂ Counteracts Mn²⁺ Toxicity—In a previous work we found that an excess of cytosolic Mn²⁺ alters mRNA transcription regulation and challenges genome stability (2). An example is the transcriptional 42-fold down-regulation of the low-affinity plasma membrane Mn²⁺ transporter *PHO84* (YML123C). Interestingly, upon CaCl₂ addition, transcriptional down-regulation of *PHO84* was reversed, suggesting that extracellular CaCl₂ alters cellular Mn²⁺ levels (see the supplemental data). To test if this is the case, we first compared the total cellular manganese and calcium levels in wild type and *pmr1Δ* cells in the presence of extracellular CaCl₂ (Fig. 1A). In accordance with previous studies (16), *pmr1Δ* cells suffered from a dramatic increase in total manganese and calcium levels. Upon the addition of CaCl₂, the cellular calcium content increased with a concurrent decrease in the manganese content (~8.5-fold). Because Mn²⁺ interferes with telomerase activity leading to telomere shortening (29) we assayed telomere length variation as an indirect measure for nuclear Mn²⁺ levels (Fig. 1B). We found that telomere shortening in *pmr1Δ* mutants was alleviated upon CaCl₂ addition, suggesting that the addition of extracellular CaCl₂ either competes with Mn²⁺ uptake or stimulates the removal of toxic Mn²⁺ from the cytoplasm.

Transformation with an *SMF1* overexpression vector challenged *pmr1Δ* viability independently of CaCl₂ supplementation (data not shown), indicating that increased Smf1 levels could lead to uncontrolled and toxic Mn²⁺ uptake. Loss of the Mn²⁺ importer Smf1 should, therefore, impair Mn²⁺ uptake and suppress *pmr1Δ* phenotypes related to cytosolic Mn²⁺ excess. However, deletion of *SMF1* has been shown to be lethal in combination with *pmr1Δ* (30) (Fig. 1C, left), whereas mutations in *PMR1* up-regulate Smf1 protein levels under Mn²⁺ starvation conditions (11). Interestingly, we could recover viable *pmr1Δ smf1Δ* spores when the tetrads were plated on CaCl₂-containing medium (Fig. 1C, right), suggesting that CaCl₂ is able to facilitate bypass of Mn²⁺ toxicity via an alternative mechanism.

Bypass of *pmr1Δ* Glycosylation Defects Requires the Putative Mn²⁺ Transporters *Spf1* and *Smf2*—Numerous studies have reported suppression of other *pmr1Δ* phenotypes by CaCl₂ (31–33). However, the underlying mechanism by which this occurs remains unclear. We asked whether other cation transporters contribute to this phenomenon. First, we set up a tar-

geted, genetic screen for synthetic phenotypes of *pmr1Δ* with deletion of genes involved in Ca²⁺ or Mn²⁺ homeostasis. As a read-out, we monitored *pmr1Δ*-dependent loss-of-viability by the cell wall-perturbing agent calcofluor white (CFW) (34, 35) and recovery-of-viability in the presence of CaCl₂. Consistent with glycosylation defects, *pmr1Δ* shows a weakened cell wall exemplified by hypersensitivity to CFW, Congo Red, and hygromycin B and constitutive activation of the cell integrity pathway (36). Notably, CaCl₂-mediated recovery of viability was not observed in other mutants affected in protein glycosylation such as *anp1Δ*, lacking a *cis*-Golgi α-1,6-mannosyltransferase subunit (Fig. 2A). Interestingly, CFW sensitivity of *pmr1Δ pho84Δ*, *pmr1Δ vcx1*, and *pmr1Δ ccc1Δ* double mutants was suppressed by CaCl₂, whereas *pmr1Δ spf1Δ* and *pmr1Δ smf2Δ* double mutants failed to grow upon CaCl₂ addition (Fig. 2B).

Mn²⁺ ions are essential cofactors for the activity of Golgi-hosted mannosyltransferases that progressively and sequentially *N*-glycosylate proteins in different Golgi compartments (18, 37). Glycosylation events along the secretory route can be followed by analyzing carboxypeptidase Y (CPY) maturation. CPY is subjected to core glycosylation in the ER (p1 form). The core oligosaccharides are extended in the Golgi by the sequential addition of α1,6-, α1,2-, and α1,3-linked mannose residues, which results in a mobility shift when analyzed by SDS-PAGE (p2 form). After delivery to the vacuole, the pro region is cleaved to yield mCPY (see Fig. 2C, left) (38). In accordance with a previous report (31), fully glycosylated CPY (p2) was nearly absent in *pmr1Δ* mutants, but CPY glycosylation recovered upon CaCl₂ addition. We confirmed the previously described CPY glycosylation defect of *pmr1Δ spf1Δ* double mutants (39), but surprisingly CPY glycosylation was significantly diminished in *smf2Δ* mutants, and even more interestingly, we observed a CaCl₂ persistent glycosylation defect in *smf2Δ*, *spf1Δ* single and *pmr1Δ smf2Δ*, *pmr1Δ spf1Δ* double mutants. To further define the protein glycosylation defect of *smf2Δ* mutants, we compared CPY mannosylation patterns by pulse-chase labeling and sequential immunoprecipitation with antibodies specific to either CPY or α1,6-mannose linkages (Fig. 2D). In contrast to *pmr1Δ*, *smf2Δ* isolated CPY can be α1,6-mannosyl-immunoprecipitated, indicating a proficient early (*cis*-Golgi) α1,6-mannosyl addition. We, therefore, searched for evidence that the *N*-glycosylation defect of *smf2Δ* cells might be linked to a late glycosylation event. Consequently, we assessed the subcellular localization of Smf2 by colocalization experiments with protein markers for the *trans*-

FIGURE 2. CaCl₂-mediated suppression of CPY glycosylation defects is *pmr1Δ*-specific and depends on the metal transporters *Spf1* and *Smf2*. A, CaCl₂ does not suppress the CFW sensitivity of mutants lacking the *cis*-Golgi α-1,6-mannosyltransferase complex subunit Anp1. WT, *pmr1Δ*, and *anp1Δ* cells were grown to mid-log phase, serially diluted, and spotted onto YPAD or YPAD + CFW (15 μg/ml) without or with the addition of 10 mM CaCl₂ in the medium. Pictures were taken after 3 days. B, CaCl₂ fails to rescue CFW resistance of *pmr1Δ* mutants in the absence of *Spf1* or *Smf2*. Shown is CFW sensitivity of *pmr1Δ* upon additional deletion of the low affinity Mn²⁺ transporter *PHO84* (12), the vesicular Mn²⁺ transporter *SMF2* (10), the vacuolar Ca²⁺/H⁺ exchanger *VCX1* (68), the plasma membrane Ca²⁺ channel *CCH1* (69), the vacuolar Fe²⁺/Mn²⁺ transporter *CCC1* (19), and the putative ER Mn²⁺-transporter *SPF1* (14). Drop test analysis of WT, *pmr1Δ*, *pho84Δ*, *pmr1Δ pho84Δ*, *smf2Δ*, *pmr1Δ smf2Δ*, *vcx1Δ*, *pmr1Δ vcx1Δ*, *cch1Δ*, *pmr1Δ cch1Δ*, *ccc1Δ*, *pmr1Δ ccc1Δ*, *spf1Δ*, and *pmr1Δ spf1Δ* cells is shown. See panel A for growth conditions. C, CaCl₂ failed to restore CPY glycosylation of *pmr1Δ* mutants in the absence of *Spf1* or *Smf2*. A schematic representation of CPY maturation is shown (left). Pulse-chase analysis of CPY maturation with or without the addition of 10 mM CaCl₂ is shown (right). Proliferating cells were radiolabeled for 5 min, chased for the indicated times, and lysed. CPY was immunoprecipitated, resolved by SDS-PAGE, and analyzed by phosphorimaging. ER (p1), Golgi (p2), and vacuole (m) CPY forms are indicated. D, *smf2Δ* mutant is proficient in the α1,6-mannosyl addition. Cells were radiolabeled for 5 min and chased for 30 min. CPY was recovered by immunoprecipitation, split into two equal aliquots, subjected to secondary immunoprecipitation with antiserum to CPY or α1,6-mannose linkages, resolved by SDS-PAGE, and subjected to phosphorimaging analysis. Ab, antibody.

Intra-Golgi Manganese Redistribution

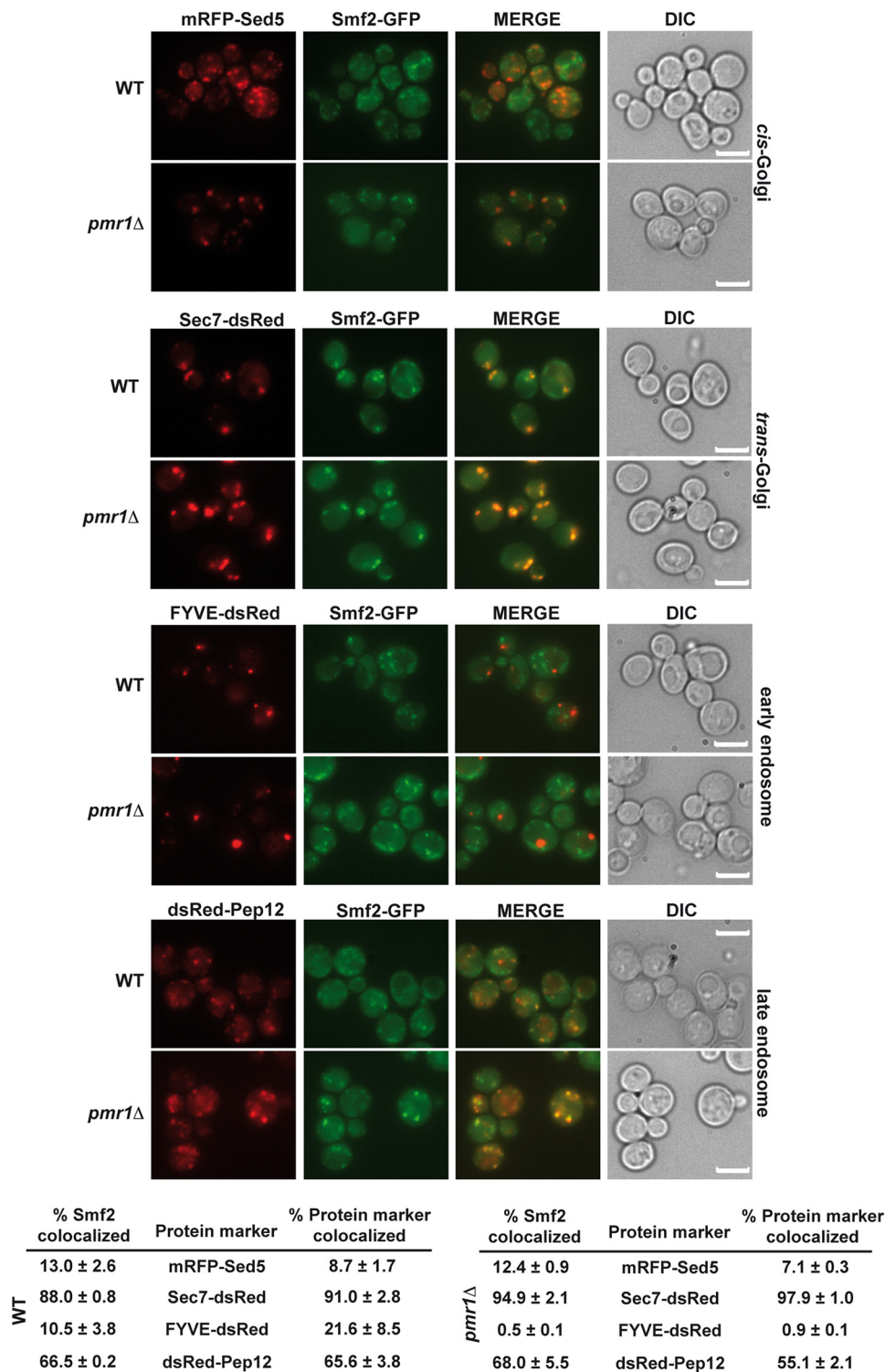


FIGURE 3. **Smf2 is primarily localized at *trans*-Golgi.** Microscopy images of WT and *pmr1*Δ cells co-expressing the chromosomal fusion protein Smf2-GFP and different tagged proteins (as indicated). Percentages of co-localization with markers for the *trans*-Golgi (Sec7), *cis*-Golgi (Sed5), early endosome (FYVE domain), or late endosome (Pep12) are indicated (*bottom*). Percentages were quantified with respect to Smf2 or the indicated marker. At least 100 cells per marker were assessed, and errors represent S.D. of three independent experiments. Bar, 5 μm.

Golgi network (Sec7), late-endosome (Pep12), *cis*-Golgi (Sed5), or early endosome (FYVE; see Fig. 3). Interestingly, microscopic analysis showed that Smf2 co-localizes with 70 and 90% of late endosome and *trans*-Golgi markers, respectively. In contrast, Smf2 poorly co-localized with *cis*-Golgi and early endosomes markers (Sed5 and FYVE, respectively). These findings

suggest that Smf2 supplies late endosome and *trans*-Golgi with Mn²⁺ and raise the question as to how Smf2 is connected to *cis*-Golgi Mn²⁺ homeostasis.

Smf2 and Atx2 Have Antagonistic Roles in Late Endosome/Trans-Golgi Mn²⁺ Transport—Another option would be that the late endosome/*trans*-Golgi could act as a cellular Mn²⁺

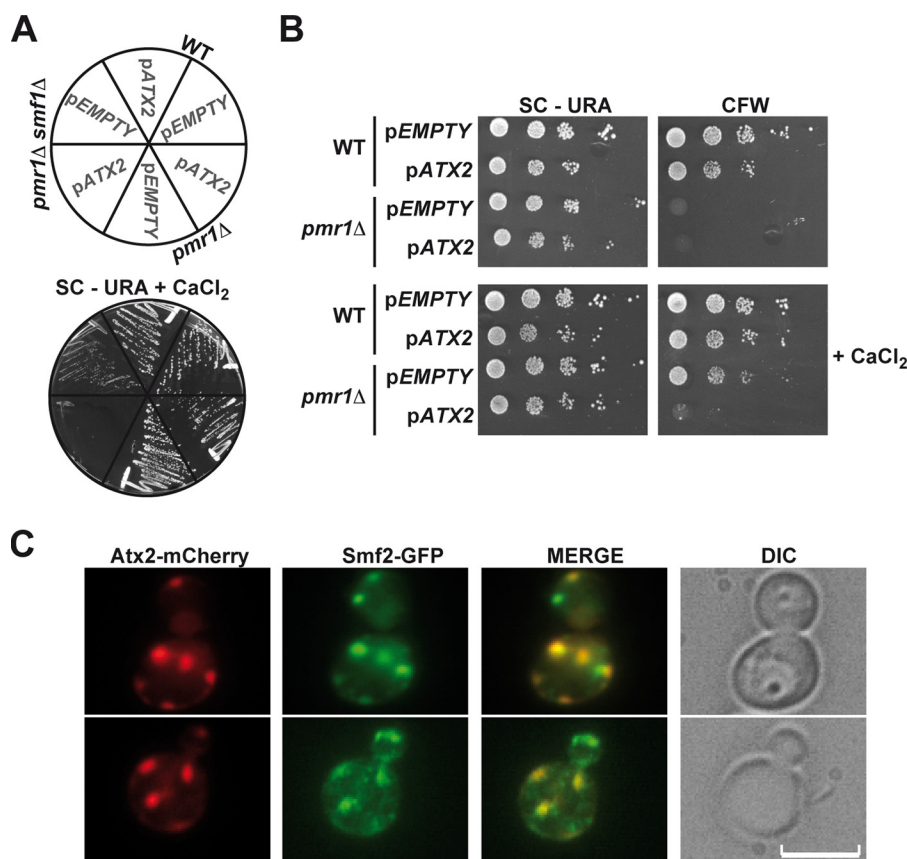


FIGURE 4. **Atx2 is a *trans*-Golgi protein that counteracts Smf2 activity.** *A*, *ATX2* overexpression annuls CaCl_2 -mediated viability of *pmr1Δ smf1Δ*. Shown is the growth of WT, *pmr1Δ* and *pmr1Δ smf1Δ* cells transformed with an empty vector (p2UGpd) or with a plasmid overexpressing *ATX2* (p*ATX2*) on SC-ura + CaCl_2 . *B*, *ATX2* overexpression compromises the CaCl_2 -mediated CFW resistance of *pmr1Δ* mutants. Drop test sensitivity of WT and *pmr1Δ* cells transformed with a plasmid overexpressing *ATX2* (p*ATX2*) or with the empty vector (p2UGpd) against CFW (15 $\mu\text{g/ml}$) without (top) or with (bottom) the addition of 10 mM CaCl_2 is shown. *C*, Atx2 (red) co-localizes with Smf2 (green) to the *trans*-Golgi. Microscopic images of WT cells co-transformed with plasmids expressing Atx2-mCherry and Smf2-GFP are shown. DIC, differential interference contrast. Bar, 5 μm .

storage compartment as previously proposed by Luk and Culotta (8). If so, we reasoned that a Mn^{2+} exporter system might be required to prevent *trans*/post-Golgi Mn^{2+} overload. A candidate for such activity is Atx2, based on the observations that Atx2 is a Golgi membrane protein whose overproduction provides the cytoplasm with antioxidative Mn^{2+} activities that compensate for the loss of cytoplasmic *SOD1*, although Atx2 effect seems to require Smf1 function (13). To validate our hypothesis, we determined if *ATX2* overexpression counteracts the CaCl_2 -mediated *pmr1Δ smf1Δ* viability (Fig. 4*A*). In fact, transformation of *pmr1Δ smf1Δ* double mutants with an *ATX2* overexpressing plasmid conferred lethality in the presence of CaCl_2 , indicating a Smf1-independent function of Atx2. In addition, *ATX2* overexpression compromised the CaCl_2 -dependent suppression of CFW sensitivity in *pmr1Δ* mutants (Fig. 4*B*). These observations suggest that Atx2 might expel Mn^{2+} from the *trans*-Golgi but also that enough Mn^{2+} is available for Atx2-mediated Mn^{2+} transport in CaCl_2 -treated *pmr1Δ smf1Δ* cells. We, therefore, determined if Atx2 and Smf2 co-localize to the same compartment (Fig. 4*C*). This was indeed the case, and based on our experimental evidence we anticipate that Smf2 and Atx2 might have antagonistic roles in *trans*-Golgi Mn^{2+} homeostasis such that Smf2 and Atx2 are required for *trans*-/post-Golgi Mn^{2+} import and export, respectively.

CaCl}_2-dependent Suppression Does Not Rely on Calcineurin-mediated Signaling or Smf2 Redistribution from *Trans*- to *Cis*-Golgi—Extracellular Ca^{2+} has been shown to initiate signal transduction events (40). The conserved Ca^{2+} /calmodulin-dependent protein phosphatase calcineurin plays a critical role in Ca^{2+} -mediated signaling (41). Therefore, we scored CFW sensitivity of *pmr1Δ* mutants compromised in the calcineurin regulatory subunit *CNB1* or added calcineurin inhibitors (FK506 or cyclosporin A (*CsA*)) to the growth media (41) (see Fig. 5*A*). Neither lack of *Cnb1* nor the addition of calcineurin inhibitors caused a loss-of-viability in the presence of CFW, suggesting that activation of calcineurin signaling is dispensable for CaCl_2 -mediated suppression of *pmr1Δ* CFW hypersensitivity.

Smf2 could have a dual role in late endosome/*trans*- and *cis*-Golgi Mn^{2+} import if one considers a CaCl_2 -dependent late endosome/*trans*- to *cis*-Golgi Smf2 redistribution. We addressed this possibility by determining the Smf2 subcellular localization in the presence of CaCl_2 and found that Smf2 still co-localized with the *trans*-Golgi marker *Sec7* but not with the *cis*-Golgi marker *Sed5* (Fig. 5*B*). Thus, the CaCl_2 -mediated suppression of *cis*-Golgi Mn^{2+} import defect in *pmr1Δ* does not occur through Smf2-mediated Mn^{2+} redistribution from *trans*- to the *cis*-Golgi.

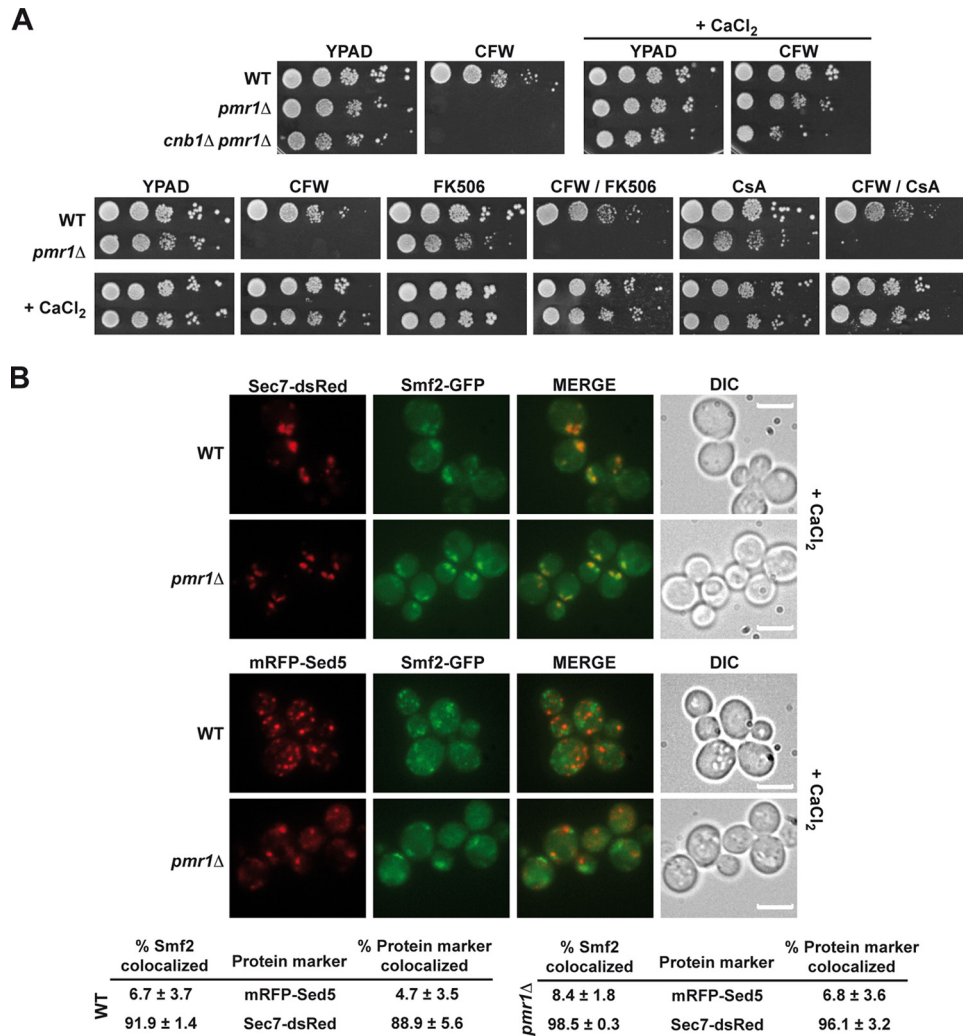


FIGURE 5. CaCl₂-mediated suppression of CFW sensitivity is not dependent on calcineurin signaling activation or trans- to cis-Golgi Smf2 redistribution. *A, top*, drop test sensitivity of WT, *pmr1*Δ, and *pmr1*Δ *cnb1*Δ against CFW (10 μg/ml) without (*left*) or with (*right*) the addition of 10 mM CaCl₂. *Bottom*, drop test sensitivity of WT and *pmr1*Δ cells against CFW (15 μg/ml), FK506 (10 μg/ml), CFW + FK506 (15 and 10 μg/ml), cyclosporin A (CsA; 50 μg/ml), and CFW/CsA (15 and 50 μg/ml) without (*top*) or with (*bottom*) the addition of 10 mM CaCl₂. *B*, microscopic images of WT and *pmr1*Δ cells co-expressing the chromosomal fusion protein Smf2-GFP and different tagged proteins (as indicated) in the presence of CaCl₂ (10 mM). *DIC*, differential interference contrast.

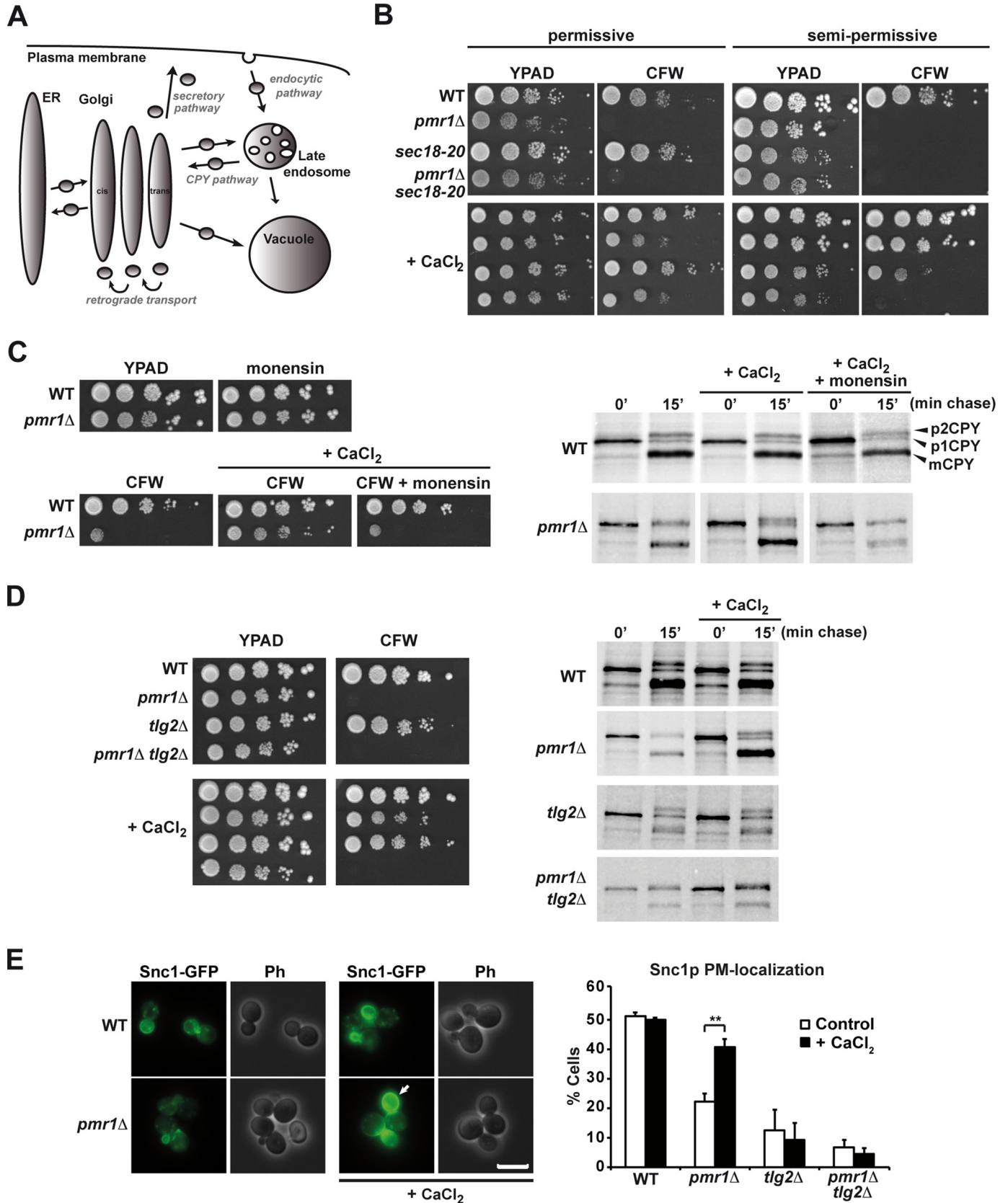
Rescue of pmr1Δ CFW Resistance Relies on a Competent Golgi Retrograde Transport Machinery—In addition to its function in cellular signaling, intracellular Ca²⁺ also plays a regulatory role in membrane trafficking. In particular, Ca²⁺ is thought to participate in different membrane fusion events within secretory and endocytic pathways including intra-Golgi transport (42) (see Fig. 6A). To determine if this is the case, we investigated whether intracellular transport and membrane fusion are essential for CaCl₂-dependent suppression of glycosylation defects. First, we benefited from a *sec18-20* mutation that has been shown to block many vesicular fusion events (43, 44). Sec18 is an essential ATPase that catalyzes the disassembly and recycling of SNARE complexes for further rounds of vesicle transport (45). Indeed, CaCl₂ failed to rescue growth of *pmr1*Δ *sec18-20* double mutants on CFW-containing media, suggesting that vesicle transport is involved in CaCl₂-dependent resistance to CFW (Fig. 6B). Next, to broadly assess vesicle trafficking steps, we took advantage of monensin, a Na⁺/H⁺ ionophore that interferes with intracellular transport by the neutralization of acidic intracellular compartments (46), block-

ing intracellular transport in both trans- and post-Golgi compartments (47). Most appealing, CaCl₂ failed to rescue the CFW resistance in the presence of monensin (Fig. 6C, *left*). We then considered that monensin constrains protein glycosylation in *pmr1*Δ mutants. This was indeed the case, as monensin suppressed the appearance of fully glycosylated CPY (p2CPY) in CaCl₂ treated *pmr1*Δ but not in WT cells (Fig. 6B, *right*).

Mn²⁺-sensitive mutants were found to be enriched in the functional category of vesicle-mediated transport including late endosome retrograde transport involving Tlg2 (48), a t-SNARE protein needed for the fusion of endosome-derived vesicles with the late Golgi (49, 50). Based on this finding we wondered if the CaCl₂-dependent suppression of CFW sensitivity and CPY glycosylation were impaired in *pmr1*Δ *tlg2*Δ double mutants. Indeed, although *tlg2*Δ mutants did not display an obvious CPY glycosylation defect, CaCl₂ could not rescue CPY glycosylation defects and viability of CFW-treated *pmr1*Δ *tlg2*Δ double mutants (Fig. 6D). To further assess the role of CaCl₂ in vesicle transport, we analyzed different mutants defective in the coatomer or COPI coat required for the forma-

tion of retrograde transport vesicles from the Golgi to the ER and between Golgi cisternae (intra-Golgi retrograde transport) (51, 52). Again, CaCl_2 failed to rescue growth of *pmr1* Δ mutants

in the absence of Sec28 and in combination with mutations of Cop1 (*ret1-1*) or Cog3 (*sec34-2*) (data not shown). Taken together, these results suggest that a functional intra-Golgi ret-



Intra-Golgi Manganese Redistribution

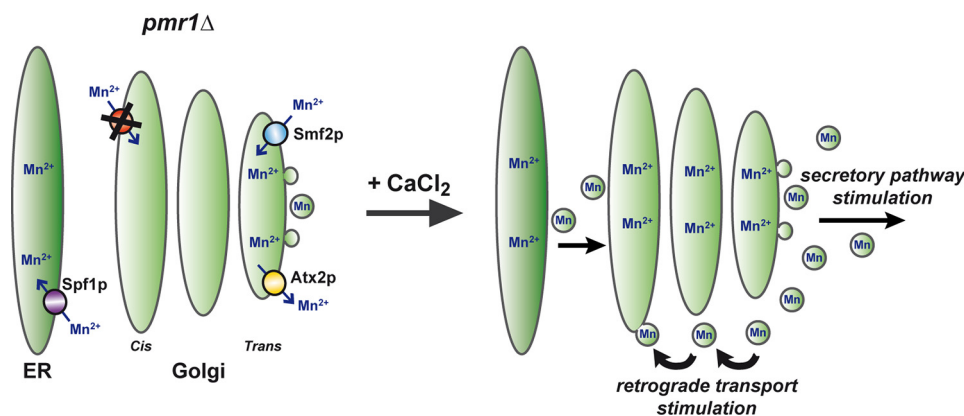


FIGURE 7. **A model for Ca^{2+} -mediated suppression of $\text{pmr1}\Delta$ -dependent phenotypes.** Lack of Pmr1 causes *cis*-Golgi manganese depletion. The addition of CaCl_2 stimulates vesicle trafficking and Mn^{2+} retrograde transport from ER to *cis*-Golgi or late endosome/*trans*- to *cis*-Golgi. *Cis*-Golgi Mn^{2+} supply restores Mn²⁺ detoxification through the secretory pathway. This model does not rule out the possibility that CaCl_2 could compete with Mn^{2+} uptake or stimulate Mn^{2+} detoxification through the secretory pathway.

rograde transport is essential for the Ca^{2+} -dependent bypass of *pmr1* Δ glycosylation defects.

Finally, to more directly assess the idea that CaCl_2 stimulates intracellular vesicle trafficking, we used the exocytic SNARE Snc1 protein to monitor protein trafficking (53). The chimeric GFP-Snc1 protein is dynamically localized at the plasma membrane by continuous endocytic recycling, via endosomes, to the *trans*-Golgi, from where it is rapidly trafficked back to the plasma membrane. It has been previously shown that GFP-Snc1 accumulates in internal structures when Golgi function is blocked (54). Consistent with a known defect in Golgi function (31), the absence of Pmr1 leads to the redistribution of GFP-Snc1 to punctuated structures (Fig. 6E). The addition of CaCl_2 restored GFP-Snc1 localization to the cell surface, suggesting that CaCl_2 indeed rescues Golgi trafficking in *pmr1* Δ mutant. By contrast, CaCl_2 addition could not restore the plasma membrane localization of GFP-Snc1 in a *tlg2* Δ mutant background, which blocks the transport of GFP-Snc1 to the Golgi from endosomes. Therefore, these results strongly suggest that CaCl_2 promotes Golgi-vesicle trafficking overcoming the lack of Pmr1.

DISCUSSION

Here we dissect a remarkable mechanism by which CaCl_2 suppresses pleiotropic phenotypes linked to impaired *cis*-Golgi manganese transport (Fig. 7; see the figure legend for an explanation). This mechanism relies on functional ER and late endosome/*trans*-Golgi Mn^{2+} transport, and we provide evidence that calcium stimulates intra-organelle Mn^{2+} redistribution through intracellular vesicle trafficking.

The P-type ATPase Spf1 and the Nramp transporter Smf2 are required for the CaCl_2 -mediated suppression of CFW sen-

sitivity and CPY glycosylation. Spf1 and Smf2 activities might be required for ER and Golgi manganese supply and thus be required for vesicle-mediated manganese transport. Recently, the Spf1 has been shown to regulate Mn^{2+} transport into the ER (14), and the addition of extracellular Ca^{2+} accordingly suppressed *SPF1* mutant phenotypes (35, 55). Smf2 was predicted to transport Mn^{2+} across membranes toward the cytosol by the assumption that Nramp transporters transport divalent cations in this direction (8). However, as is the case of Nramp1, the direction of the metal flux is still controversial (56). Thus, some authors propose that Nramp1 functions as a pH-dependent proton/divalent cation antiporter delivering divalent metal ions into acidic compartments (57–59). Accordingly, Nramp1, but not Nramp2, can rescue the metal ion stress phenotype of yeast mutants, suggesting that both proteins differ in the direction of transport (60). Notably, when expressed in yeast, Nramp1 localizes to the ER (data not shown) and thereby is unlikely to complement the transport activity of *trans*-Golgi-localized Smf2. Unfortunately, in contrast to other ions, studies on the abundance and intracellular distribution of manganese are hampered by the lack of chemical or genetically encoded manganese reporters (61).

In this work we specifically localize Smf2 in the late endosome/*trans*-Golgi, and based on our results, we believe that Smf2 might supply the *trans*-Golgi with Mn^{2+} needed for the activity of mannosyltransferases such as Mnn1 (37, 62). Neutralization of acidic *trans*- and *post*-Golgi compartments by monensin might alter Smf2 flux direction and, therefore, compromise CaCl_2 -dependent alleviation of CFW sensitivity. In addition, mutations in the vacuolar-type H^+ -transporting

FIGURE 6. **Functional vesicle trafficking/fusion is essential for CaCl_2 -dependent rescue of $\text{pmr1}\Delta$ glycosylation defects.** A, illustration of the endomembrane system. Organelles (ER, Golgi, endosome, and vacuole) and secretory, endocytic, and CPY pathways are depicted. B, drop test sensitivity of WT, *pmr1* Δ , *sec18-20*, and *pmr1* Δ *sec18-20* against CFW (10 $\mu\text{g/ml}$) without (top) or with (bottom) the addition of 10 mM CaCl_2 . Cells were grown in permissive (23 °C, left) or semi-permissive (29 °C, right) conditions. C, monensin, a drug that blocks intracellular transport, counteracts CaCl_2 -dependent suppression of glycosylation defects. Left, WT and *pmr1* Δ cells were spotted onto YPAD, monensin (25 $\mu\text{g/ml}$), CFW (10 $\mu\text{g/ml}$), CFW + CaCl_2 (10 mM), and CFW + CaCl_2 + monensin. Right, pulse-chase analysis of CPY maturation in WT and *pmr1* Δ cells without or with the addition of CaCl_2 (10 mM) or CaCl_2 + monensin (40 $\mu\text{g/ml}$). ER (p1), Golgi (p2), and vacuole (m) CPY forms are indicated. D, *pmr1* Δ mutants grown in the presence of CaCl_2 remain glycosylation deficient in the absence of Tlg2. Left, drop test sensitivity of WT, *pmr1* Δ , *tlg2* Δ and *pmr1* Δ *tlg2* Δ cells against CFW (10 $\mu\text{g/ml}$) without (top) or with (bottom) the addition of CaCl_2 (10 mM). Right, pulse-chase analysis of CPY maturation with or without the addition of CaCl_2 (10 mM). E, CaCl_2 rescues Snc1 protein trafficking. Plasma membrane localization of Snc1-GFP was quantified in WT, *pmr1* Δ , *tlg2* Δ and *pmr1* Δ *tlg2* Δ cells grown without (white bars) or with the addition of CaCl_2 (10 mM, black bars). Bar, 5 μm . Error bars represent S.D. Double asterisks (**) indicate $p < 0.01$. Phase contrast (Ph) and Snc1-GFP images are shown.

ATPase (V-ATPase), which alter Golgi acidification, share multiple *pmr1Δ* phenotypes (33). We find that Smf2 co-localizes with Atx2, a poorly characterized, putative *trans*-Golgi Mn²⁺ transporter that could function in pumping Mn²⁺ in the opposite direction to Smf2. Evidence for Atx2 ion transport activity is based on the observation that the protein shares functional characteristics with the SLC39 family of metal ion transporters (63). Consequently, Smf2 and Atx2 might form part of a late endosome/*trans*-Golgi Mn²⁺ import/export system required for a stable equilibrium between Mn²⁺ and other ions in the late endosome/*trans*-Golgi.

Regulation of Mn²⁺ homeostasis is highly conserved between yeast and higher eukaryotes, and Mn²⁺ transport enhancing mutations in the human ortholog of *PMR1*, *ATP2C1* can protect mammalian cells from the cytotoxic effects of Mn²⁺ (64). The contribution of defective Mn²⁺ transport on Hailey-Hailey disease progression is still under debate. However, increasing evidence points to the possibility that impaired manganese homeostasis triggers keratinocyte differentiation (6) and causes genetic instability (2).

We first anticipated that CaCl₂-dependent suppression of *pmr1Δ* phenotypes could involve signal transduction pathways. However, this seem not to be the case, as CaCl₂-mediated rescue of *pmr1Δ* is not coupled to Ca²⁺/calmodulin-dependent changes in gene expression or protein re-localization. Increasing evidence links Ca²⁺ to the regulation of membrane trafficking and fusion events (65, 66). The precise mechanism by which calcium regulates membrane trafficking is still poorly understood. It has been proposed that transiently released luminal calcium is required to trigger the last stages of membrane fusion (23). Accordingly, the addition of CaCl₂ suppresses the vacuole fragmentation phenotype of *pmr1Δ* mutants (33). In addition, calcium might also regulate the formation of intra-Golgi retrograde transport vesicles as it has been shown to stabilize COPI coat onto the Golgi membrane (67). The addition of CaCl₂ caused a significant increase in the intracellular calcium levels and might account for a permanent induction of retro- and anterograde pathways. Along this line, we found that CaCl₂ decreased intracellular manganese levels and restored Golgi-to-cell surface recycling of the exocytic SNARE Snc1-GFP chimera in *pmr1Δ* but not in *pmr1Δ tlg2Δ* mutants. These results point to the possibility that CaCl₂ promotes Golgi to *trans*-Golgi network, to secretory vesicle, to plasma membrane trafficking of vesicles. Based on our data we suggest that Mn²⁺-containing vesicles might emerge from the *trans*- or post-Golgi and fuse with the *cis*-Golgi, supplying the *cis*-Golgi with essential Mn²⁺ for the action of sugar transferases. Consequently, Ca²⁺ may also stimulate retro- and anterograde trafficking between later secretory pathway organelles and the ER. The results of this study raise the possibility that stimulation of vesicle transport in human cells can bypass *ATP2C1* disease phenotypes or, yet more interestingly, can counteract neurotoxicity upon manganese exposure.

Acknowledgments—We thank Drs. H. Gaillard and D. Fitzgerald for critical reading, Dr. M. Cabrera for advice, and Drs. R. Rao, H. Riezman, K. D. Hirschi, C. Ungermann, and H. Pelham for materials.

REFERENCES

- Crowley, J. D., Traynor, D. A., and Weatherburn, D. C. (2000) Enzymes and proteins containing manganese: an overview. *Met. Ions Biol. Syst.* **37**, 209–278
- García-Rodríguez, N., Díaz de la Loza Mdel, C., Andreson, B., Monje-Casas, F., Rothstein, R., and Wellinger, R. E. (2012) Impaired manganese metabolism causes mitotic misregulation. *J. Biol. Chem.* **287**, 18717–18729
- Olanow, C. W. (2004) Manganese-induced parkinsonism and Parkinson's disease. *Ann. N.Y. Acad. Sci.* **1012**, 209–223
- Brown, D. R., Hafiz, F., Glasssmith, L. L., Wong, B. S., Jones, I. M., Clive, C., and Haswell, S. J. (2000) Consequences of manganese replacement of copper for prion protein function and proteinase resistance. *EMBO J.* **19**, 1180–1186
- Missiaen, L., Raeymaekers, L., Dode, L., Vanoevelen, J., Van Baelen, K., Parys, J. B., Callewaert, G., De Smedt, H., Segart, S., and Wuytack, F. (2004) SPCA1 pumps and Hailey-Hailey disease. *Biochem. Biophys. Res. Commun.* **322**, 1204–1213
- Yoshida, M., Yamasaki, K., Daiho, T., Iizuka, H., and Suzuki, H. (2006) ATP2C1 is specifically localized in the basal layer of normal epidermis and its depletion triggers keratinocyte differentiation. *J. Dermatol. Sci.* **43**, 21–33
- Supek, F., Supekova, L., Nelson, H., and Nelson, N. (1996) A yeast manganese transporter related to the macrophage protein involved in conferring resistance to mycobacteria. *Proc. Natl. Acad. Sci. U.S.A.* **93**, 5105–5110
- Luk, E. E., and Culotta, V. C. (2001) Manganese superoxide dismutase in *Saccharomyces cerevisiae* acquires its metal co-factor through a pathway involving the Nramp metal transporter, Smf2p. *J. Biol. Chem.* **276**, 47556–47562
- Liu, X. F., and Culotta, V. C. (1999) Post-translation control of Nramp metal transport in yeast. Role of metal ions and the BSD2 gene. *J. Biol. Chem.* **274**, 4863–4868
- Portnoy, M. E., Liu, X. F., and Culotta, V. C. (2000) *Saccharomyces cerevisiae* expresses three functionally distinct homologues of the nramp family of metal transporters. *Mol. Cell Biol.* **20**, 7893–7902
- Jensen, L. T., Carroll, M. C., Hall, M. D., Harvey, C. J., Beese, S. E., and Culotta, V. C. (2009) Down-regulation of a manganese transporter in the face of metal toxicity. *Mol. Biol. Cell* **20**, 2810–2819
- Jensen, L. T., Aja-Alemanji, M., and Culotta, V. C. (2003) The *Saccharomyces cerevisiae* high affinity phosphate transporter encoded by PHO84 also functions in manganese homeostasis. *J. Biol. Chem.* **278**, 42036–42040
- Lin, S. J., and Culotta, V. C. (1996) Suppression of oxidative damage by *Saccharomyces cerevisiae* ATX2, which encodes a manganese-trafficking protein that localizes to Golgi-like vesicles. *Mol. Cell Biol.* **16**, 6303–6312
- Cohen, Y., Megyeri, M., Chen, O. C., Condomitti, G., Riezman, I., Loizides-Mangold, U., Abdul-Sada, A., Rimon, N., Riezman, H., Platt, F. M., Futerman, A. H., and Schuldiner, M. (2013) The yeast p5 type ATPase, spf1, regulates manganese transport into the endoplasmic reticulum. *PLoS ONE* **8**, e85519
- Rudolph, H. K., Antebi, A., Fink, G. R., Buckley, C. M., Dorman, T. E., LeVitre, J., Davidow, L. S., Mao, J. I., and Moir, D. T. (1989) The yeast secretory pathway is perturbed by mutations in *PMR1*, a member of a Ca²⁺ ATPase family. *Cell* **58**, 133–145
- Lapinskas, P. J., Cunningham, K. W., Liu, X. F., Fink, G. R., and Culotta, V. C. (1995) Mutations in *PMR1* suppress oxidative damage in yeast cells lacking superoxide dismutase. *Mol. Cell Biol.* **15**, 1382–1388
- Mandal, D., Woolf, T. B., and Rao, R. (2000) Manganese selectivity of *pmr1*, the yeast secretory pathway ion pump, is defined by residue Gln-783 in transmembrane segment 6. Residue Asp-778 is essential for cation transport. *J. Biol. Chem.* **275**, 23933–23938
- Dürr, G., Strayle, J., Plemper, R., Elbs, S., Klee, S. K., Catty, P., Wolf, D. H., and Rudolph, H. K. (1998) The medial-Golgi ion pump Pmr1 supplies the yeast secretory pathway with Ca²⁺ and Mn²⁺ required for glycosylation, sorting, and endoplasmic reticulum-associated protein degradation. *Mol. Biol. Cell* **9**, 1149–1162
- Li, L., Chen, O. S., McVey Ward, D., and Kaplan, J. (2001) CCC1 is a

- transporter that mediates vacuolar iron storage in yeast. *J. Biol. Chem.* **276**, 29515–29519
20. Beckers, C. J., and Balch, W. E. (1989) Calcium and GTP: essential components in vesicular trafficking between the endoplasmic reticulum and Golgi apparatus. *J. Cell Biol.* **108**, 1245–1256
 21. Porat, A., and Elazar, Z. (2000) Regulation of intra-Golgi membrane transport by calcium. *J. Biol. Chem.* **275**, 29233–29237
 22. Mayorga, L. S., Berón, W., Sarrouf, M. N., Colombo, M. I., Creutz, C., and Stahl, P. D. (1994) Calcium-dependent fusion among endosomes. *J. Biol. Chem.* **269**, 30927–30934
 23. Peters, C., and Mayer, A. (1998) Ca^{2+} /calmodulin signals the completion of docking and triggers a late step of vacuole fusion. *Nature* **396**, 575–580
 24. Sheff, M. A., and Thorn, K. S. (2004) Optimized cassettes for fluorescent protein tagging in *Saccharomyces cerevisiae*. *Yeast* **21**, 661–670
 25. Niedenthal, R. K., Riles, L., Johnston, M., and Hegemann, J. H. (1996) Green fluorescent protein as a marker for gene expression and subcellular localization in budding yeast. *Yeast* **12**, 773–786
 26. Snaith, H. A., Samejima, I., and Sawin, K. E. (2005) Multistep and multi-mode cortical anchoring of tea1p at cell tips in fission yeast. *EMBO J.* **24**, 3690–3699
 27. Pittman, J. K., Cheng, N. H., Shigaki, T., Kunta, M., and Hirschi, K. D. (2004) Functional dependence on calcineurin by variants of the *Saccharomyces cerevisiae* vacuolar $\text{Ca}^{2+}/\text{H}^{+}$ exchanger Vcx1p. *Mol. Microbiol.* **54**, 1104–1116
 28. Peyroche, A., Courbeyrette, R., Rambourg, A., and Jackson, C. L. (2001) The ARF exchange factors Gea1p and Gea2p regulate Golgi structure and function in yeast. *J. Cell Sci.* **114**, 2241–2253
 29. Lue, N. F., Bosoy, D., Moriarty, T. J., Autexier, C., Altman, B., and Leng, S. (2005) Telomerase can act as a template- and RNA-independent terminal transferase. *Proc. Natl. Acad. Sci. U.S.A.* **102**, 9778–9783
 30. Paidhungat, M., and Garrett, S. (1998) Cdc1 is required for growth and Mn^{2+} regulation in *Saccharomyces cerevisiae*. *Genetics* **148**, 1777–1786
 31. Antebi, A., and Fink, G. R. (1992) The yeast Ca^{2+} -ATPase homologue, PMR1, is required for normal Golgi function and localizes in a novel Golgi-like distribution. *Mol. Biol. Cell* **3**, 633–654
 32. Funakoshi, M., Kajiwara, R., Goda, T., Nishimoto, T., and Kobayashi, H. (2000) Isolation and characterisation of a mutation in the PMR1 gene encoding a Golgi membrane ATPase, which causes hypersensitivity to over-expression of Clb3 in *Saccharomyces cerevisiae*. *Mol. Gen. Genet.* **264**, 29–36
 33. Yadav, J., Muend, S., Zhang, Y., and Rao, R. (2007) A phenomics approach in yeast links proton and calcium pump function in the Golgi. *Mol. Biol. Cell* **18**, 1480–1489
 34. Ram, A. F., Wolters, A., Ten Hoopen, R., and Klis, F. M. (1994) A new approach for isolating cell wall mutants in *Saccharomyces cerevisiae* by screening for hypersensitivity to calcofluor white. *Yeast* **10**, 1019–1030
 35. Suzuki, C., and Shimma, Y. I. (1999) P-type ATPase spf1 mutants show a novel resistance mechanism for the killer toxin SMKT. *Mol. Microbiol.* **32**, 813–823
 36. Bates, S., MacCallum, D. M., Bertram, G., Munro, C. A., Hughes, H. B., Buurman, E. T., Brown, A. J., Odds, F. C., and Gow, N. A. (2005) *Candida albicans* Pmr1p, a secretory pathway P-type $\text{Ca}^{2+}/\text{Mn}^{2+}$ -ATPase, is required for glycosylation and virulence. *J. Biol. Chem.* **280**, 23408–23415
 37. Dean, N. (1999) Asparagine-linked glycosylation in the yeast Golgi. *Biochim. Biophys. Acta* **1426**, 309–322
 38. Stevens, T., Esmon, B., and Schekman, R. (1982) Early stages in the yeast secretory pathway are required for transport of carboxypeptidase Y to the vacuole. *Cell* **30**, 439–448
 39. Vashist, S., Frank, C. G., Jakob, C. A., and Ng, D. T. (2002) Two distinctly localized p-type ATPases collaborate to maintain organelle homeostasis required for glycoprotein processing and quality control. *Mol. Biol. Cell* **13**, 3955–3966
 40. Hofer, A. M., and Brown, E. M. (2003) Extracellular calcium sensing and signalling. *Nat. Rev. Mol. Cell Biol.* **4**, 530–538
 41. Cyert, M. S. (2003) Calcineurin signaling in *Saccharomyces cerevisiae*: how yeast go crazy in response to stress. *Biochem. Biophys. Res. Commun.* **311**, 1143–1150
 42. Chen, J. L., Ahluwalia, J. P., and Stamnes, M. (2002) Selective effects of calcium chelators on anterograde and retrograde protein transport in the cell. *J. Biol. Chem.* **277**, 35682–35687
 43. Graham, T. R., and Emr, S. D. (1991) Compartmental organization of Golgi-specific protein modification and vacuolar protein sorting events defined in a yeast sec18 (NSF) mutant. *J. Cell Biol.* **114**, 207–218
 44. Riezman, H. (1985) Endocytosis in yeast: several of the yeast secretory mutants are defective in endocytosis. *Cell* **40**, 1001–1009
 45. Mayer, A., Wickner, W., and Haas, A. (1996) Sec18p (NSF)-driven release of Sec17p (α -SNAP) can precede docking and fusion of yeast vacuoles. *Cell* **85**, 83–94
 46. Murén, E., Oyen, M., Barmark, G., and Ronne, H. (2001) Identification of yeast deletion strains that are hypersensitive to brefeldin A or monensin, two drugs that affect intracellular transport. *Yeast* **18**, 163–172
 47. Dinter, A., and Berger, E. G. (1998) Golgi-disturbing agents. *Histochem. Cell Biol.* **109**, 571–590
 48. Chesi, A., Kilaru, A., Fang, X., Cooper, A. A., and Gitler, A. D. (2012) The role of the Parkinson's disease gene PARK9 in essential cellular pathways and the manganese homeostasis network in yeast. *PLoS ONE* **7**, e34178
 49. Raths, S., Rohrer, J., Crausaz, F., and Riezman, H. (1993) end3 and end4: two mutants defective in receptor-mediated and fluid-phase endocytosis in *Saccharomyces cerevisiae*. *J. Cell Biol.* **120**, 55–65
 50. Abeliovich, H., Grote, E., Novick, P., and Ferro-Novick, S. (1998) Tlg2p, a yeast syntaxin homolog that resides on the Golgi and endocytic structures. *J. Biol. Chem.* **273**, 11719–11727
 51. Wuestehube, L. J., Duden, R., Eun, A., Hamamoto, S., Korn, P., Ram, R., and Schekman, R. (1996) New mutants of *Saccharomyces cerevisiae* affected in the transport of proteins from the endoplasmic reticulum to the Golgi complex. *Genetics* **142**, 393–406
 52. Duden, R., Kajikawa, L., Wuestehube, L., and Schekman, R. (1998) epsilon-COP is a structural component of coatomer that functions to stabilize α -COP. *EMBO J.* **17**, 985–995
 53. Robinson, M., Poon, P. P., Schindler, C., Murray, L. E., Kama, R., Gabriely, G., Singer, R. A., Spang, A., Johnston, G. C., and Gerst, J. E. (2006) The Gcs1 Arf-GAP mediates Snc1,2 v-SNARE retrieval to the Golgi in yeast. *Mol. Biol. Cell* **17**, 1845–1858
 54. Lewis, M. J., Nichols, B. J., Prescianotto-Baschong, C., Riezman, H., and Pelham, H. R. (2000) Specific retrieval of the exocytic SNARE Snc1p from early yeast endosomes. *Mol. Biol. Cell* **11**, 23–38
 55. Cronin, S. R., Khoury, A., Ferry, D. K., and Hampton, R. Y. (2000) Regulation of HMG-CoA reductase degradation requires the P-type ATPase Cod1p/Spf1p. *J. Cell Biol.* **148**, 915–924
 56. Nevo, Y., and Nelson, N. (2006) The NRAMP family of metal-ion transporters. *Biochim. Biophys. Acta* **1763**, 609–620
 57. Atkinson, P. G., and Barton, C. H. (1999) High level expression of Nramp1G169 in RAW264.7 cell transfectants: analysis of intracellular iron transport. *Immunology* **96**, 656–662
 58. Zwilling, B. S., Kuhn, D. E., Wikoff, L., Brown, D., and Lafuse, W. (1999) Role of iron in Nramp1-mediated inhibition of mycobacterial growth. *Infect Immun.* **67**, 1386–1392
 59. Goswami, T., Bhattacharjee, A., Babal, P., Searle, S., Moore, E., Li, M., and Blackwell, J. M. (2001) Natural-resistance-associated macrophage protein 1 is an H^{+} /bivalent cation antiporter. *Biochem. J.* **354**, 511–519
 60. Techau, M. E., Valdez-Taubas, J., Popoff, J. F., Francis, R., Seaman, M., and Blackwell, J. M. (2007) Evolution of differences in transport function in Slc11a family members. *J. Biol. Chem.* **282**, 35646–35656
 61. Rimón, N., and Schuldiner, M. (2011) Getting the whole picture: combining throughput with content in microscopy. *J. Cell Sci.* **124**, 3743–3751
 62. Graham, T. R., Seeger, M., Payne, G. S., MacKay, V. L., and Emr, S. D. (1994) Clathrin-dependent localization of α 1,3 mannosyltransferase to the Golgi complex of *Saccharomyces cerevisiae*. *J. Cell Biol.* **127**, 667–678
 63. Eide, D. J. (2004) The SLC39 family of metal ion transporters. *Pflügers Arch.* **447**, 796–800
 64. Mukhopadhyay, S., and Linstedt, A. D. (2011) Identification of a gain-of-function mutation in a Golgi P-type ATPase that enhances Mn^{2+} efflux and protects against toxicity. *Proc. Natl. Acad. Sci. U.S.A.* **108**, 858–863
 65. Hu, K., Carroll, J., Fedorovich, S., Rickman, C., Sukhodub, A., and Davletov, B. (2002) Vesicular restriction of synaptobrevin suggests a role for calcium in membrane fusion. *Nature* **415**, 646–650

66. Hay, J. C. (2007) Calcium: a fundamental regulator of intracellular membrane fusion? *EMBO Rep.* **8**, 236–240
67. Ahluwalia, J. P., Topp, J. D., Weirather, K., Zimmerman, M., and Stamnes, M. (2001) A role for calcium in stabilizing transport vesicle coats. *J. Biol. Chem.* **276**, 34148–34155
68. Cunningham, K. W., and Fink, G. R. (1996) Calcineurin inhibits VCX1-dependent H^+/Ca^{2+} exchange and induces Ca^{2+} ATPases in *Saccharomyces cerevisiae*. *Mol. Cell Biol.* **16**, 2226–2237
69. Paidhungat, M., and Garrett, S. (1997) A homolog of mammalian, voltage-gated calcium channels mediates yeast pheromone-stimulated Ca^{2+} uptake and exacerbates the *cdc1(Ts)* growth defect. *Mol. Cell Biol.* **17**, 6339–6347
70. Proszynski, T. J., Klemm, R. W., Gravert, M., Hsu, P. P., Gloor, Y., Wagner, J., Kozak, K., Grabner, H., Walzer, K., Bagnat, M., Simons, K., and Walch-Solimena, C. (2005) A genome-wide visual screen reveals a role for sphingolipids and ergosterol in cell surface delivery in yeast. *Proc. Natl. Acad. Sci. U.S.A.* **102**, 17981–17986
71. Markgraf, D. F., Ahnert, F., Arlt, H., Mari, M., Peplowska, K., Epp, N., Griffith, J., Reggiori, F., and Ungermann, C. (2009) The CORVET subunit Vps8 cooperates with the Rab5 homolog Vps21 to induce clustering of late endosomal compartments. *Mol. Biol. Cell* **20**, 5276–5289
72. Matsuura-Tokita, K., Takeuchi, M., Ichihara, A., Mikuriya, K., and Nakano, A. (2006) Live imaging of yeast Golgi cisternal maturation. *Nature* **441**, 1007–1010